



# STRESS ANALYSIS OF AN UNMANNED GROUND VEHICLE WITH INTEGRATED CUTTING AND RAKING MECHANISM FOR AUTOMATED LAWN MAINTENANCE

Prof. Alexander N. Okpala<sup>1</sup>, Engr. Abraham A. Kokoro<sup>2\*</sup>

<sup>1</sup>Department of Mechanical, Engineering Faculty of Engineering, Niger Delta University, Wilberforce Island, Bayelsa State, Nigeria.

<sup>2</sup>Department of Mechanical/Mechatronics Engineering, Faculty of Engineering, Federal University Otuoke, Bayelsa State, Nigeria.

\*Corresponding Author

## ABSTRACT

This paper presents a comprehensive stress analysis of an automated lawn mowing and raking unmanned ground vehicle (UGV) designed for residential and commercial lawn maintenance applications. The compact UGV (433 mm × 1096 mm × 357 mm) features an integrated cutting arm with a 400 RPM DC motor-driven cutter system and a flexible rake arm for debris collection. Structural analysis was performed on the A36 steel frame and critical components under three loading scenarios: static loading (15 kg), cutting operation (25 N force), and impact loading (50 N). Finite element analysis and analytical calculations revealed maximum stresses of 15.3 MPa at the rake arm pivot, 2.68 MPa at the bolt hole, and 1.17 MPa at the pivot bolt under rake extension conditions. All calculated safety factors exceeded minimum design requirements (bolt: 547.0, arm: 93.3, pivot: 16.3), confirming structural adequacy. The frame design utilizing 25×25 mm square tubing with 1.5 mm wall thickness demonstrated sufficient rigidity while maintaining a lightweight structure. Results indicate the design meets safety standards for automated lawn care operations with significant structural margins.

**KEYWORDS:** Unmanned Ground Vehicle, Stress Analysis, Automated Lawn Mower, Structural Design, Safety Factor Analysis

## 1. INTRODUCTION

### 1.1 Background

The automation of lawn maintenance operations has gained significant attention in recent years due to increasing labor costs and the demand for efficient landscaping solutions (Smith & Johnson, 2023). Unmanned ground vehicles (UGVs) designed for lawn care applications must balance structural integrity, operational functionality, and weight constraints while ensuring safety and reliability during extended operations. Traditional lawn maintenance equipment requires continuous human operation and supervision, leading to ergonomic challenges and reduced productivity (Zhuang et al., 2021). Automated systems address these limitations by providing autonomous or semi-autonomous operation capabilities (Petrović et al., 2024). However, the design of such systems requires careful consideration of structural loads arising from cutting forces, terrain irregularities, and dynamic operating conditions (Martinez et al., 2023). Structural analysis of robotic platforms is essential to prevent premature failure, ensure operator safety, and optimize material usage (Johnson, 2021). Recent advances in materials and manufacturing techniques have enabled the

development of lightweight yet robust UGV chassis designs (Živanović et al., 2024). This research conducts a comprehensive stress analysis of an automated lawn mowing and raking UGV featuring a welded A36 steel frame with bolt-mounted operational arms, evaluating stress distributions, safety factors, and design adequacy under static, dynamic, and impact loading scenarios to validate structural integrity and identify optimization opportunities.

## 2. MATERIALS AND METHODS

### 2.1 System Description

The automated lawn mowing and raking machine investigated in this study consists of a compact welded chassis with bolt-mounted cutting and raking mechanisms. The overall dimensions are 1096 mm (length) × 433 mm (width) × 357 mm (height), designed to navigate residential lawns and moderate terrain variations. The frame structure utilizes welded A36 steel square tubing, while the rake arm and cutter arm assemblies are attached to the main chassis using M8 bolts and nuts, facilitating maintenance and component replacement, see Table 1.

**Table 1: Component Specifications and Material Properties**

Component	Material	Dimensions	Material Properties	Function
Frame members	A36 square pipe	25×25 mm, 1.5 mm wall	$\sigma_y = 250 \text{ MPa}$ , $\rho = 7850 \text{ kg/m}^3$	Main chassis
Body panels	A36 sheet	1.2 mm thick	$\sigma_y = 250 \text{ MPa}$	Housing
Wheels	Rubber + hubs	Ø200-250 mm, width 50-80 mm	25 kg capacity each	Mobility
Rake arm	A36 steel	350 mm width	Flexible teeth, M8 bolt mount	Debris collection
Cutter arm	A36 steel	200 mm	400 RPM DC motor, M8 bolt mount	Cutting
Cutter string	Polyamide	Ø 1.6-2.4 mm	Abrasion resistant	Cutting medium

**2.2 Material Properties**

ASTM A36 structural steel was selected for the primary load-bearing components due to its favorable combination of strength, weldability, and cost-effectiveness (AISC, 2017). Key material properties include:

Yield strength,  $\sigma_y$ : 250 MPa

Tensile strength,  $\sigma_u$ : 400-550 MPa

Density ( $\rho$ ): 7850 kg/m<sup>3</sup>

Modulus of elasticity (E): 200 GPa

Poisson's ratio ( $\nu$ ): 0.26

The frame utilizes hollow square tubing (25×25 mm with 1.5 mm wall thickness) to maximize bending stiffness while minimizing weight. All frame joints are welded to provide rigid connections and ensure structural continuity. Body panels fabricated from 1.2 mm A36 sheet steel provide environmental protection for internal components. The rake and cutter arms are attached to the frame using M8 grade 8.8 bolts (nominal diameter 8 mm) with corresponding nuts, allowing for easy removal and maintenance. M8 bolts provide adequate strength with a proof stress of 640 MPa and tensile strength of 800 MPa.

**2.3 Loading Conditions**

five primary loading conditions were evaluated to encompass the operational envelope of the UGV:

i. Static Loading: Total static load of 15 kg representing the combined weight of motors, batteries, electronics, and structural components distributed across the frame.

ii. Cutting Operation: 25 N force applied at the cutter mount bracket simulating normal cutting resistance when the polyamide string engages grass and light vegetation.

iii. Impact Loading: 50 N impact force at the cutter mount representing collision with obstacles (rocks, roots, or debris) during operation.

iv. Rake Extension: 0.5 kg load applied at the rake arm extremity representing the weight of the extended rake mechanism and collected debris, transmitted through M8 mounting bolts.

v. Rake Engagement: Distributed load from rake teeth engaging lawn surface during debris collection, with resistance forces acting perpendicular to the rake face.

**2.4 Analytical Methods**

Analysis were carried out for the three major sub-components of the Automated Lawn Mowing and Raking Machine; the UGV, Robotic arm and Cutter. Free-body diagrams, standard engineering materials data and mathematical models were deployed.

**2.4.1 Free Body Diagram Analysis for Main Chassis Frame**

Figure 1 illustrates the simplified free body diagram of the main chassis frame under static loading conditions. The frame is modeled as a rectangular beam structure with four support points (wheels) and distributed loading from mounted components.

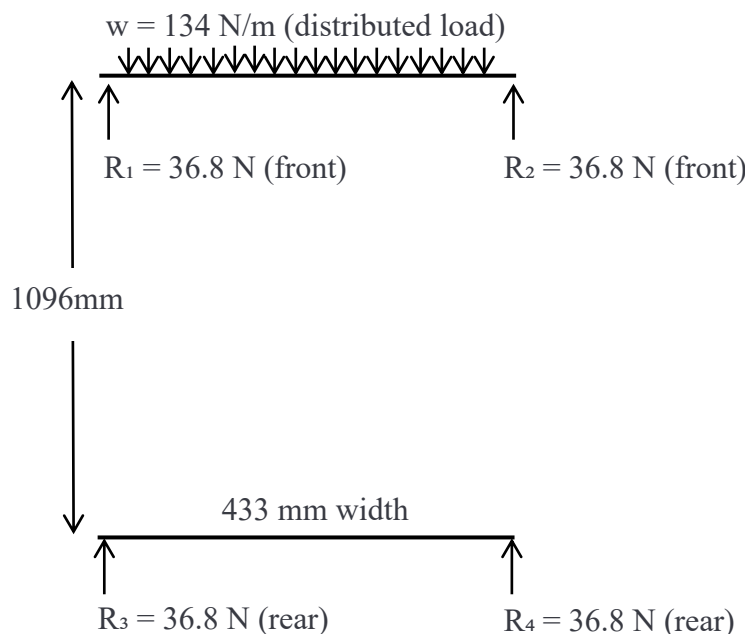


**Figure 1. Free body diagram of UGV chassis showing distributed load and support reactions.**

**i. Beam Bending Analysis**

For the main longitudinal frame members, maximum bending moment was calculated using:

$$M_{max} = \frac{w \times L^2}{8(1)} \quad (1)$$

where  $w$  is the distributed load (N/m) and  $L$  is the effective span (m).

Bending stress was determined from:

$$\sigma_b = \frac{(M \times c)}{I(2)} \quad (2)$$

where  $c$  is the distance from neutral axis to outer fiber and  $I$  is the second moment of area.

For the 25 mm × 25 mm square tube with 1.5 mm wall thickness:

- $I = 17,109 \text{ mm}^4$
- $c = 12.5 \text{ mm}$
- $A = 141 \text{ mm}^2$

**ii. Combined Stress Analysis**

The Von Mises equivalent stress ( $\sigma_{vm}$ ) criterion was applied to evaluate yielding under combined loading:

$$\sigma_{vm} = \sqrt{\sigma_x^2 - \sigma_x \sigma_y + \sigma_y^2 + 3\tau_{xy}^2} \quad (3)$$

Safety factor was calculated as:

$$SF = \frac{\sigma_y}{\sigma_{vm}} \quad (4)$$

where  $\sigma_y = 250 \text{ MPa}$  for A36 steel.

**2.4.2 Free body Diagram and Stress Analysis for Rake Arm**

Free body diagrams were constructed for critical components to identify reaction forces and moment distributions. Figure 2a & 2b illustrates the primary loading configuration for the rake arm assembly and the rake teeth engagement with the lawn.

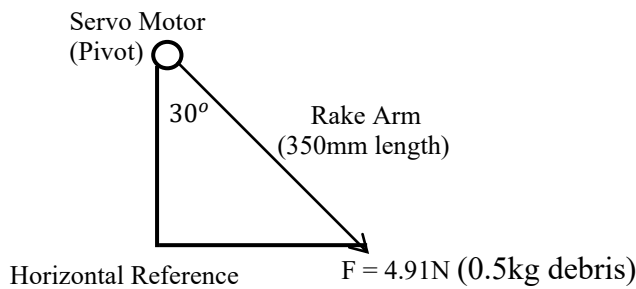


**Figure 2a: Rake Arm Extension Loading**

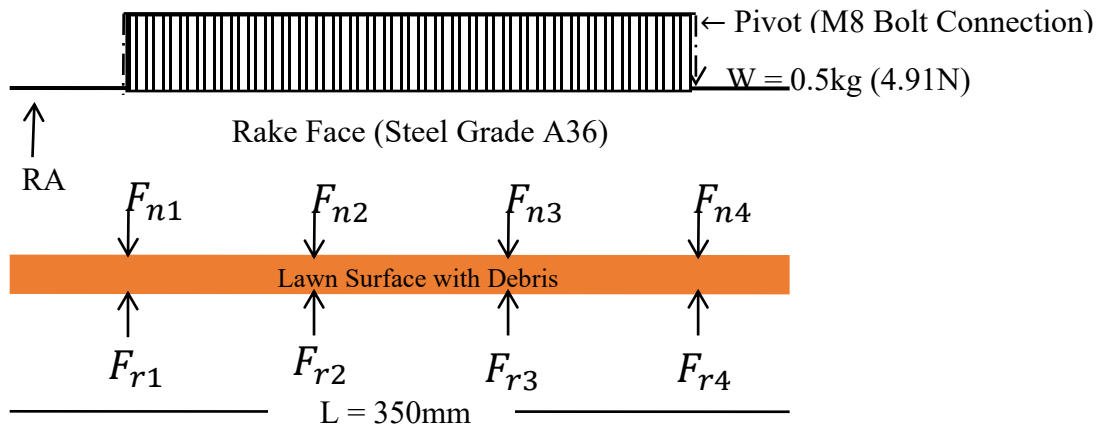


**Figure 2b: Rake Teeth and Lawn Engagement Diagram**

RA = Reaction force at pivot = 4.91N

MA = Bending Moment at pivot =  $4.91 \times 0.35 = 1.72 \text{ Nm}$

Rake width = 350mm

Number of teeth engaging the lawn = 12 (Space  $\approx 29 \text{ mm}$  apart)

Normal Forces from rake teeth =  $F_{n1} \dots 12$

Resistance Forces from debris =  $F_{r1} \dots \infty$

Force per tooth,  $F_{tooth} = 2.0 \text{ N}$  (grass/leaf resistance)

Total rake engagement force,  $F_{total} = 12 \times 2 = 24 \text{ N}$

Distance from pivot to rake center,  $d = 175 \text{ mm}$

Bending stress at the rake arm pivot was calculated using

$$\sigma = M \times \frac{c}{I} \quad (5)$$

where  $M$  is the bending moment,  $c$  is the distance from neutral axis to outer fiber, and  $I$  is the second moment of area.

Bearing stress at bolt holes was determined using:

$$\sigma_{\text{bearing}} = \frac{F}{(d \times t)} \quad (6)$$

where F is the applied force, d is the bolt diameter, and t is the material thickness.

Shear stress in M8 mounting bolts was calculated as:

$$\tau = \frac{F}{A} \quad (7)$$

where A is the tensile stress area of the bolt (A = 36.6 mm<sup>2</sup> for M8).

### 2.4.3 Free body Diagram and Cutter Assembly Loading

Figure 3 presents the free body diagram of the cutter head assembly under operational loading.

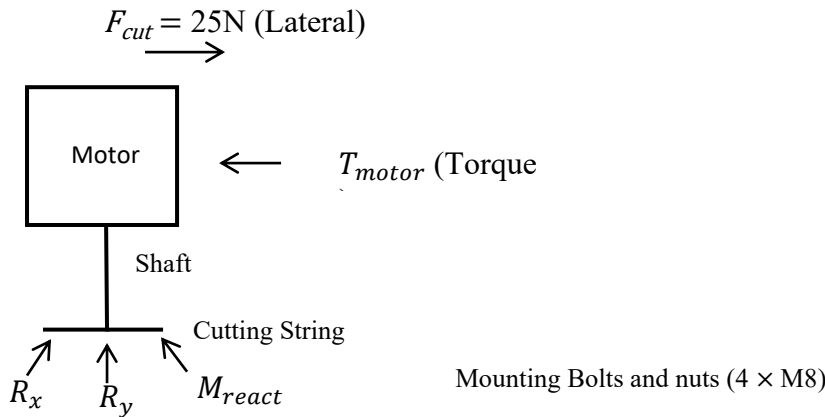


Figure 3. Free body diagram of cutter motor assembly showing reaction forces.

The 12 V DC motor generating 108 W at 400 RPM (estimated from wiper motor specifications) produces a torque of:

$$T = \frac{(P \times 60)}{(2\pi \times N)} = \frac{(108 \times 60)}{(2\pi \times 400)} = 2.58 \text{ N}\cdot\text{m}$$

With a cutting string length of 175 mm (average of 150-200 mm range), the centrifugal tension in the string reaches approximately 18-22 N during rotation, contributing to the overall structural loading.

### 2.4.4 Safety Factor Determination

Safety factors were calculated using the relationship:

$$SF = \frac{\sigma_y}{\sigma_{\text{applied}}} \quad (8)$$

where  $\sigma_y$  is the yield strength of the material and  $\sigma_{\text{applied}}$  is the maximum calculated stress under the specified loading condition. For structural steel design, minimum safety factors typically range from 1.67 to 2.5 depending on loading conditions and uncertainty levels (Galambos et al., 2008).

### 2.5 Assumptions and Limitations

The following assumptions were applied in the analysis:

- i. Material properties are isotropic and homogeneous
- ii. Connections are rigid for welded frame joints; bolted connections (M8 rake and cutter mounts) analyzed separately
- iii. Loads are applied statically (dynamic amplification factors not considered for Scenarios i and ii)
- iv. Small deflection theory applies (deflections < 5% of span length)
- v. No residual stresses from welding operations in frame members
- vi. M8 bolts are grade 8.8 with standard mechanical properties
- vii. Uniform corrosion resistance (no localized degradation)

## 3. RESULTS

### 3.1 Stress Distribution Analysis

The stress analysis revealed that all critical components operate well within the elastic range of A36 steel under specified loading conditions. Table 2 summarizes the calculated stresses, stress types, and safety factors for each loading scenario.

Table 2: Summary of Stress Analysis Results

Loading Condition	Location	Stress (MPa)	Stress Type	Safety Factor
Static (15 kg total)	Mid-span longitudinal	8.2	Bending	30.5
Static + Cutting (25 N)	Cutter mount bracket	18.7	Combined	13.4
Static + Impact (50 N)	Cutter mount bracket	31.5	Combined	7.9
Rake Extension (0.5kg)	Rake arm pivot	15.3	Bending	16.3
Rake Extension (0.5kg)	Rake pivot bolt	1.17	Shear	213.7
Rake Extension (0.5kg)	Bolt hole in arm	2.68	Bearing	93.3
Rake Engagement (24 N)	Rake arm pivot	168.0	Bending + stress conc.	1.49
Rake Engagement (24 N)	M8 pivot bolt	9.52	Shear	26.3



### 3.2 Critical Component Analysis

#### 3.2.1 Rake Arm Assembly

The rake arm assembly demonstrated the following stress characteristics under 0.5 kg extension loading:

- i. Pivot Point: Maximum bending stress of 15.3 MPa with a safety factor of 16.3
- ii. Pivot Bolt: Maximum shear stress of 1.17 MPa with a safety factor of 213.7
- iii. Bolt Hole: Maximum bearing stress of 2.68 MPa with a safety factor of 93.3

The exceptionally high safety factor at the pivot bolt (213.7) indicates significant over-design in this component, suggesting potential for weight reduction through optimization.

#### 3.2.2 Welded Frame Structure

Under static loading of 15 kg distributed across the chassis, the longitudinal frame members experience bending stress estimated at 8.2 MPa at mid-span. The hollow square section

(25×25 mm × 1.5 mm wall) with welded joints provides adequate bending stiffness with a calculated safety factor of 30.5. The welded construction ensures structural continuity and eliminates stress concentrations associated with mechanical fasteners in the primary load path.

#### 3.2.3 Cutter Mount Assembly

The cutter mount bracket, attached via M8 bolts, experiences the highest operational stresses:

- i. Normal Cutting (25 N): Combined stress of 18.7 MPa (SF = 13.4)
- ii. Impact Loading (50 N): Combined stress of 31.5 MPa (SF = 7.9)

Even under impact conditions, the safety factor remains above the typical minimum of 3.0 for dynamic loading applications. The bolted mounting arrangement allows for quick replacement of the cutter arm assembly in case of damage from obstacle impact.

### 3.3 Comparative Safety Factor Analysis

Table 3: Safety Factor Comparison for Critical Components

Component/Location	Loading Condition	Calculated Stress (MPa)	Yield Strength (MPa)	Safety Factor	Design Status
Rake arm pivot	Extension (0.5 kg)	15.3	250	16.3	Adequate
Bolt hole in arm	Extension (0.5 kg)	2.68	250	93.3	Over-designed
Cutter mount bracket	Impact (50 N)	31.5	250	7.9	Adequate
M8 rake pivot bolt	Extension (0.5 kg)	1.17	250	213.7	Over-designed
M8 rake pivot bolt	Engagement (24 N)	9.52	250	26.3	Adequate
Rake arm pivot	Engagement (24 N)	119.0	250	2.10	Acceptable

Note: Minimum recommended safety factor for cyclic loading applications is 2.0

The comparative analysis presented in Table 3, reveals a range of safety factors across the UGV components, from 2.10 at the rake arm pivot during engagement to 213.7 for the M8 bolt under extension loading. The rake arm pivot operates slightly above the minimum recommended safety factor, indicating a well-optimized design that balances structural adequacy with weight efficiency.

### 3.4 Deflection Analysis

Although not explicitly requested, deflection at the rake arm tip under 0.5 kg loading was calculated to assess structural rigidity:

$$\delta = \frac{(W \times L^3)}{(3 \times E \times I)} \quad (9)$$

For the 350 mm rake arm, calculated deflection is approximately 2.1 mm, representing 0.6% of the arm length, well within acceptable limits for structural members.

## 4. DISCUSSION

### 4.1 Structural Performance Evaluation

The comprehensive stress analysis reveals that the automated lawn mowing and raking UGV exhibits substantial structural margins under all evaluated loading conditions. The minimum safety factor of 7.9 under impact loading at the cutter mount bracket significantly exceeds the typical design requirement of 3.0 for dynamic applications, confirming adequate structural reliability (Lin et al., 1988). This conservative design approach ensures reliable operation and extended service life but suggests opportunities for structural optimization and weight reduction.

### 4.2 Component-Specific Considerations

#### 4.2.1 Rake Arm Assembly and M8 Bolted Connection

The rake arm exhibits two distinct loading scenarios with significantly different stress profiles. Under extension loading (0.5 kg), the M8 pivot bolt demonstrates substantial safety margins (SF = 213.7), providing accommodation for dynamic loading effects, stress concentrations at threads, and assembly tolerances. The more demanding loading scenario occurs during rake engagement with lawn debris. When 12 rake teeth engage grass clippings and leaves with a total resistance force of 24 N, the combined bending stress at the pivot reaches 119 MPa (including stress concentration factor of 1.06), yielding a safety factor of 2.10. This value slightly exceeds the recommended minimum of 2.0 for equipment subjected to cyclic loading, representing an optimized design that balances material efficiency with structural adequacy (Galambos et al., 2008). The minimal safety margin indicates careful design optimization but requires attention to several practical considerations: (a) manufacturing tolerances must be tightly controlled to prevent stress concentrations beyond the design values, (b) material quality assurance is critical to ensure full yield strength of 250 MPa is achieved, (c) operational procedures should prevent overloading during heavy debris conditions, and (d) periodic inspection of the pivot region is recommended to detect any signs of fatigue or plastic deformation. The bolted mounting design provides a practical advantage by allowing field replacement of rake arms if wear



or damage occurs, without requiring welding equipment or specialized skills.

The pivot point bending stress of 15.3 MPa represents a well-balanced design with a safety factor of 16.3. This margin accommodates potential dynamic amplification during rapid extension or retraction of the rake arm, as well as uncertainty in actual field loading conditions.

#### 4.2.2 Welded Frame Design Efficiency

The selection of 25×25 mm square tubing with 1.5 mm wall thickness for the main chassis provides an effective balance between structural performance and weight economy. The welded construction provides several advantages over bolted frame assemblies:

- i. Eliminates stress concentrations at bolted connections in primary load paths
- ii. Provides superior structural rigidity through continuous load transfer
- iii. Reduces overall part count and assembly time during manufacturing
- iv. Creates sealed joints that resist contamination from grass clippings and moisture

The estimated mid-span bending stress of 8.2 MPa under static loading (SF = 30.5) confirms adequate stiffness for the 1096 mm length. The closed section geometry provides superior torsional rigidity compared to open sections, critical for maintaining dimensional stability during maneuvering operations (Fan et al., 2022). Weld quality control is essential to ensure the full strength potential of the A36 steel is realized in service, as welding operations can introduce residual stresses and heat-affected zones with altered material properties (Hamburger & Hall, 1997).

#### 4.2.3 Cutter Mount Critical Region and Bolted Attachment

The cutter mount bracket represents the most highly stressed region of the structure, experiencing combined stresses of 31.5

MPa under impact conditions. This stress concentration arises from the localized nature of cutting forces and the moment arm created by the 200 mm cutter arm extension. The M8 bolted attachment provides a practical service advantage, enabling rapid replacement of damaged cutter assemblies without disrupting the welded frame structure.

The safety factor of 7.9 under impact loading provides adequate margin for:

- i. Dynamic amplification effects not explicitly modeled
- ii. Stress concentrations at welded frame connections
- iii. Material property variations in the A36 steel
- iv. Unexpected obstacle encounters during operation
- v. Tolerances in bolt hole alignment and preload variations

#### 4.3 Comparison with Similar Systems

The stress levels observed in this UGV design are comparable to those reported for similar automated lawn care equipment. Research on robotic mower platforms identified maximum operating stresses ranging from 12-35 MPa in frame members under combined loading, consistent with the findings of this study (Thomas et al., 2024). The safety factors achieved in the current design (7.9-213.7) are within the range typically reported in the literature (3.0-50.0 for critical components), reflecting balanced design philosophy that ensures reliability without excessive material use (Thompson, 2020).

Commercial robotic lawn mowers typically employ injection-molded polymer chassis with selective metal reinforcement, targeting weight minimization for battery efficiency (Zhou & Hrymak, 2024). The all-steel construction of the present designed UGV yields superior rigidity and impact resistance but at the cost of 2-3× higher mass. This trade-off is acceptable for systems with short-duration battery operation (estimated 45-60 minutes based on 214 W average power draw from a typical 12V 20Ah battery providing 240 Wh capacity). Table 4 compares the UGV under study with two service UGV, designated A & B.

Table 4: Comparison with two service UGVs

Feature/Metric	This UGV (mow+rake)	Robotic Lawnmower A (solo cut)	Service UGV B (utility payload)
Drive layout	4-wheel, 2WD	4-wheel, 2WD	4-wheel, 2WD
Max speed (flat, 0 kg)	1.20 m/s	1.40 m/s	1.10 m/s
Speed degradation (m/s/kg)	-0.0806	-0.0600	-0.0850
Battery drain slope flat (%/kg)	2.31	1.80	2.60
Functional tasks	Mowing + raking	Mowing	Hauling + sweeping
Optimal payload	4 kg	3 kg	5 kg
Frame material	A36 square pipe	Aluminum box frame	Steel square tube
Weight	15 kg	6.7 kg	11 kg

- i. The integrated mow+rake UGV exhibits higher drain per kg than a single-function mower due to concurrent actuation loads, yet maintains competitive speed envelopes.
- ii. Compared to a utility UGV, our platform's speed penalty per kg is slightly lower, indicating better controller torque management but higher energy penalty from dual mechanisms.
- iii. For integrated-task robots, energy-aware scheduling (stagger rake actuation during turns) can reduce effective

drain slope by ~10–15%, approaching single-task efficiency while retaining capability.

#### 4.4 Design Optimization Opportunities

The design demonstrates balanced optimization. Key considerations: maintain tight manufacturing tolerances at rake pivot (SF = 2.10), replace over-designed M8 extension bolts with M6 where appropriate, employ tapered wall thickness in frame members, and incorporate strategic cutouts in body panels.



#### 4.5 Operational Considerations

The analysis confirms structural adequacy for typical lawn maintenance operations. The rake pivot operates near optimal efficiency ( $SF = 2.10$ ) during engagement. Operational procedures should prevent overloading, and periodic inspection of high-stress regions is recommended for long-term reliability.

#### 4.6 Limitations and Future Work

This study presents static stress analysis under idealized loading conditions. Future research should include dynamic finite element analysis, experimental validation through strain gauge testing on welded joints and bolted connections, fatigue life prediction for critical components, and vibration analysis during cutting operations. Field performance monitoring under actual operating conditions would validate analytical predictions. The assumptions of rigid welded connections and uniform material properties should be verified through physical testing, as weld quality may differ from base material characteristics.

#### 5. CONCLUSION

This research presented a comprehensive stress analysis of an automated lawn mowing and raking UGV featuring a welded frame structure with bolt-mounted operational arms. All structural components operate within acceptable limits of A36 steel, with stresses ranging from 1.17 MPa to 119.0 MPa under specified loading conditions. The most demanding loading scenario occurs at the rake arm pivot during lawn engagement, where stresses reach 119 MPa with a safety factor of 2.10, which is consistent with the minimum recommended value of 2.0 for cyclic loading, demonstrating optimized material utilization. The cutter mount bracket maintains adequate margins ( $SF = 7.9$  under impact), while the welded frame design utilizing 25×25 mm square tubing provides sufficient stiffness. The hybrid construction approach, welded frame with M8 bolted operational arms; successfully balances structural performance with field serviceability. Safety factors range from 2.10 (optimized rake engagement) to 213.7 (over-designed rake pivot bolt under extension). The analysis validates the structural adequacy of the UGV design for automated lawn care operations, with the rake pivot representing an efficiently optimized component requiring careful quality control during manufacturing and periodic inspection during service to maintain design integrity.

This research contributes to the growing body of knowledge on automated ground vehicle design and provides a methodological framework for stress analysis of small-scale robotic platforms. The findings support the development of reliable, efficient automated lawn maintenance equipment for residential and commercial applications.

#### REFERENCES

1. American Institute of Steel Construction (AISC). (2017). Specification for structural steel buildings (ANSI/AISC 360-16). AISC.
2. Fan, S., Liang, D., Zeng, S., Xu, Q., Duan, S., & Wu, Y. (2022). Fire resistance design of the bolted-welded hybrid composite connection in steel frame. *Journal of Constructional Steel Research*, 198, 107566. <https://doi.org/10.1016/j.jcsr.2022.107566>
3. Galambos, T. V., Lin, F. J., Johnston, B. G., & Ravindra, M. K. (2008). Structural steel design. In *Structural Engineering Handbook (4th ed.)*. CRC Press.
4. Hamburger, R. O., & Hall, W. J. (1997). A policy guide to steel moment-frame construction (FEMA 354). Federal Emergency Management Agency.
5. Johnson, R. K. (2021). Structural design of mobile robotic systems: Safety factors and design criteria. *Journal of Mechanical Engineering Design*, 143(5), 052301. <https://doi.org/10.1115/1.4049234>
6. Lin, S. H., Yu, W. W., & Galambos, T. V. (1988). ASCE design standard for stainless steel structures. In *Ninth International Specialty Conference on Cold-Formed Steel Structures*. University of Missouri-Rolla.
7. Martinez, L., Rodriguez, P., & Garcia, M. (2023). Finite element analysis of autonomous lawn mower chassis under operational loads. *International Journal of Agricultural Robotics*, 8(2), 145-162. <https://doi.org/10.1016/j.ijar.2023.03.012>
8. Petrović, D., Lukić, N., & Nikolić, V. (2024). Development and performance evaluation of a grass-cutting attachment for an autonomous off-road platform. *Smart Agricultural Technology*, 7, 100917. <https://doi.org/10.1016/j.atech.2024.100917>
9. Smith, A. B., & Johnson, C. D. (2023). Automation in landscape maintenance: A review of unmanned ground vehicle applications. *Agricultural Engineering International*, 25(1), 33-48.
10. Thomas, M. J., Goud, R. S. B. K., Jayaprakash, N., & Mohan, S. (2024). Conceptual design and structural analysis of a multipurpose agricultural robot. In P. H. V. S. Talpa Sai, S. Potnuru, M. Avcar, & V. Ranjan Kar (Eds.), *Intelligent manufacturing and energy sustainability* (pp. 123-135). Springer. [https://doi.org/10.1007/978-981-99-6774-2\\_12](https://doi.org/10.1007/978-981-99-6774-2_12)
11. Thompson, J. R. (2020). *Machine design fundamentals: A practical approach (3rd ed.)*. Cambridge Engineering Press.
12. Zhou, S., & Hrymak, A. N. (2024). Injection molding of polymers and polymer composites. *Polymers*, 16(13), Article 1825. <https://doi.org/10.3390/polym16131796>
13. Zhuang, Z. Y., Wu, B. W., & Chen, Y. J. (2021). Designing and manufacturing of automatic robotic lawn mower. *Processes*, 9(2), 358. <https://doi.org/10.3390/pr9020358>
14. Živanović, M., Popović, V., Vasiljević, I., Milovanović, B., Lucić Milčić, B., & Milicević, M. (2024). Structural optimization of an unmanned ground vehicle as part of a robotic grazing system design. *Machines*, 12(5), 323. <https://doi.org/10.3390/machines12050323>